Modular Injectable Matrices Based on Alginate Solution/Microsphere Mixtures That Gel *in situ* and Co-Deliver Immunomodulatory Factors

Yuki Hori[a], **Amy M. Winans**[a,b], and **Darrell J. Irvine**[a,b,c,d,*]

[a]Department of Materials Science and Engineering, Massachusetts Institute of Technology, Cambridge MA, 02139

[b]Department of Biological Engineering, Massachusetts Institute of Technology, Cambridge MA, 02139

[c]Koch Institute for Integrative Cancer Research

[d]Howard Hughes Medical Institute

Abstract

Biocompatible polymer solutions that can crosslink *in situ* following injection to form stable hydrogels are of interest as depots for sustained delivery of therapeutic factors or cells, and as scaffolds for regenerative medicine. Here, injectable self-gelling alginate formulations obtained by mixing alginate microspheres (as calcium reservoirs) with soluble alginate solutions were characterized for potential use in immunotherapy. Rapid redistribution of calcium ions from microspheres into the surrounding alginate solution led to rapid crosslinking and formation of stable hydrogels. The mechanical properties of the resulting gels correlated with the concentration of calcium reservoir microspheres added to the solution. Soluble factors such as the cytokine interleukin-2 were readily incorporated into self-gelling alginate matrices by simply mixing them with the formulation prior to gelation. Using alginate microspheres as modular components, strategies for binding immunostimulatory CpG oligonucleotides onto the surface of microspheres were also demonstrated. When injected subcutaneously in the flanks of mice, self-gelling alginate formed soft macroporous gels supporting cellular infiltration and allowing ready access to microspheres carrying therapeutic factors embedded in the matrix. This in-situ gelling formulation may thus be useful for stimulating immune cells at a desired locale such as solid tumors or infection sites as well as for other soft tissue regeneration applications.

Keywords

Alginate; injectable hydrogel; controlled release; immobilized factors; cell infiltration

Introduction

Alginate is a natural polysaccharide commonly obtained from brown seaweed, which forms a physical hydrogel in the presence of divalent cations such as calcium. Due to its biocompatibility, mildness of gelation conditions, and low immunogenicity, purified alginate has been widely used in food and pharmaceutical industries, as well as for many

*Corresponding author. Department of Materials Science and Engineering and Department of Biological Engineering, Massachusetts Institute of Technology, Cambridge, MA, 02139. djirvine@mit.edu. Tel: 617-452-4174; fax: 617-452-3293.

biomedical, biomaterial, and therapeutic applications [1-5]. Alginate chains are multiblock copolymers consisting of poly-D-mannuronic acid (M) blocks, poly-L-guluronic acid (G) blocks, and alternating G/M blocks. The size, proportions, and the distribution of each block influence both the physical and chemical properties of alginate, with G units contributing to the crosslinking capacity through stereocomplexation in an "egg-box" conformation[6], while M and G/M blocks provide flexibility to the resulting networks. Alginate is stable against breakdown by mammalian enzymes but dissolves and can be eliminated through the kidneys *in vivo*; alternatively, partial oxidation of uronic units of sodium alginate can be used to make alginate susceptible to hydrolytic breakdown *in vivo* [7,8][9].

Because of the cooperative nature of crosslinking by G units and the small size of the crosslinking ions, gelation of alginate can occur very rapidly. For example, aqueous alginate solutions added dropwise into a calcium-containing aqueous bath form gel beads via rapid diffusion of calcium into the alginate. Such 'external gelation' methods have been employed for entrapment of cells or macromolecules into microbeads for therapeutic agent delivery [2,3,10]. Alternatively, 'internal' gelation methods have been developed, in which the gelling ions are supplied from within an initially soluble alginate solution. For example, calcium salts with low water solubility, such as carbonate, sulfate, and phosphate [1,11-14] can be mixed with alginate precursor solutions; slow dissolution of these inorganic calcium sources controllably crosslinks the surrounding alginate solution. Since many calcium salts and complexed ions show pH-dependent solubility, molecules such as polyphosphate or ethylenediamine tetraacetic acid (EDTA) [11,15,16] or chloride compounds such as ammonium chloride[15] may be added to alginate solutions to promote gradual release of calcium by changing the pH of the release medium.

To achieve non-invasive delivery of alginate gels for biomedical applications, variations on the concept of internal gelation have been employed to create 'self-gelling' formulations of alginate that facilitate injection of alginate followed by *in situ* crosslinking *in vivo*. Melvic et al [17] lyophilized calcium alginate gels and milled these dried solids to form calcium alginate particles, which were used as a source of slowly-released calcium ions when mixed with soluble alginate solutions. Thermally triggered release of calcium from phospholipid vesicles mixed with alginate solutions, employing liposomes that rupture at a physiological temperature, has also been demonstrated as a method for *in situ* formation of alginate hydrogels [18]. Alternatively, for applications where soft gels are suitable, alginate with low levels of calcium added can be formulated as a viscous solution that is still injectable [X].

Recently, we developed a self-gelling alginate hydrogel formulation based on alginate microspheres as calcium reservoirs mixed with soluble alginate solutions [19]. When calcium-reservoir microspheres were mixed with alginate/cell solutions and injected *s.c.* in mice, these solutions formed stable gels *in vivo* within ~60 min. In our initial studies [19], we explored the use of these injectable gels for delivery of dendritic cells (DCs), key immune cells capable of initiating immune responses for vaccination or immunotherapy in cancer or infectious diseases [20-25]. DCs sequestered in alginate gels elicited robust recruitment of host T-cells and dendritic cells to the matrix, and the induction of immune responses by these 'vaccination nodes' was demonstrated. T-cells primed in the native lymph nodes trafficked to these alginate gels, indicating that this DC-gel immunization is capable of directing effector T-cells to defined tissue sites in large numbers.

To build on these initial studies and better understand how the composition of injectable alginate gels influences their properties, here we focus on the gel materials themselves and report characterization of the mechanical properties and structure of gels formed from self-gelling alginate formulations *in vitro* and *in vivo*. Compositions were chosen such that the gels form low-viscosity solutions amenable to mixing/drawing in a syringe, and set to form

stable gels following injection via crosslinks contributed by ions in the interstitial fluid *in vivo*. A similar strategy of injecting of low-viscosity calcium-crosslinked alginate (via homogenization and dispersion of calcium gluconate in a sodium alginate solution) followed by gelation *in situ* has also been successfully employed for repair of myocardial infarction in rats in a recent study by Landa, et al[26]. In addition, we explored strategies to enhance the function of these gels in immunotherapy, via the co-delivery of the immunomodulatory factors interleukin-2 (IL-2) and CpG oligonucleotides in the matrix. We thus demonstrate two different strategies for incorporating factors into these injectable matrices, encapsulation within the bulk matrix (IL-2), or electrostatic anchoring to the surfaces of embedded alginate microspheres (CpG oligos). By variable combination of these strategies, a flexible platform for cell delivery and supporting factors is obtained. This modular approach to augmenting an injectable, biocompatible gel that supports cellular infiltration with slow release of cytokines or presentation of factors immobilized within the matrix may be useful in a range of soft tissue regenerative medicine applications, in addition to our particular interest in immunotherapy of cancer.

Materials and Methods

Materials

Sterile alginates Pronova SLM20 (MW 75,000 – 220,000 g/mol, >50% M units; endotoxin level <25EU/g) and Pronova SLG20 (MW 75,000 – 220,000 g/mol, >60% G units; endotoxin level <25EU/g) were purchased from Novamatrix (FMC Biopolymers, Sandvika, Norway). All antibodies were purchased from BD Biosciences (San Jose, CA). 2, 2, 4-trimethylpentane (isooctane, ChromAR grade, 99.5% purity) was obtained from Mallinckrodt Baker (Phillipsburg, NJ). Poly-L-lysine hydrobromide (MW 30,000-70,000 g/mol), FITC-poly-L-lysine hydrobromide (MW 30,000-70,000 g/mol), and 6-aminofluorescein were obtained from Sigma-Aldrich (St. Louis, MO). Mag-fura-2 tetrapotassium salt, was purchased from Invitrogen (Carlsbad, CA). CpG oligonucleotides with a phosphorothioate backbone (CpG 1826, sequence 5′-/5AmMC6/TCC ATGACGTTCCTGACGTT-3′) and FITC-CpG (FITC-CpG 1826, sequence 5′-/5AmMC6/TCC ATGACGTTCCTGACGTT/36-FAM/-3′) were synthesized by Integrated DNA Technologies (Coralville, IA). Recombinant murine IL-2 was purchased from Peprotech Inc (Rocky Hill, NJ). Hilyte Fluor™ 647 amine was purchased from Anaspec, Inc (San Jose, CA), and Slide-A-Lyzer Dialysis Cassettes (7000MWCO) from Pierce Biotechnology (Rockford, IL). All other chemicals were purchased from Sigma and used as received unless otherwise stated.

Fluorescent labeling of alginate

SLM20 alginate (0.02g/mL) was mixed with 9 mM EDC (1-Ethyl-3-[3-dimethylaminopropyl]carbodiimide hydrochloride) and 9 mM sulfo-NHS (*N*-hydroxysulfo succinimide) in PBS at 20°C for 2 hrs. An equal volume of 6-aminofluorescein (4.5 mM in 70% ethanol) or Hilyte Fluor 647 (0.32 mM in water) was added to the alginate solution containing EDC/Sulfo-NHS and reacted at 20°C for 18 hrs while rotating. The resulting solution was then dialyzed (7 KDa MWCO) against 1 L PBS at 4°C for 3 days with 3-5 changes of the dialysis bath. Labeled alginate solution was adjusted to a concentration of 0.01g/mL in PBS, sterile-filtered and stored in the dark at 4°C until use.

Calcium reservoir microsphere synthesis and self-gelling alginate

Alginate microspheres were synthesized as previously described[19], with 1.5 mL sorbitan monooleate, 0.5 mL polyethylene glycol sorbitan monooleate, and 35 mL isooctane, homogenized for 3 min using an UltraTurrax T25 homogenizer (IKA Works, Wilmington, NC) at a speed of 8×1000/min. Pronova SLG20 solution (0.01 g/mL in PBS, 400 μL) was

added and homogenized for 3 min, followed by addition of 25 μL aq. $CaCl_2$ (0.05 g/mL) with homogenization for 4 min. The resulting particles were washed once with 30 mL isooctane and 3× with 1 mL of deionized, distilled (DD) water, then resuspended in DD water for a final volume of 1 mL and stored at 4°C until use. Microsphere sizes were determined from optical micrographs taken with a Zeiss Axiovert 200 epifluorescence microscope at 40× and analyzed with MetaMorph software (Molecular Devices, Downingtown, PA). Endotoxin levels in the microspheres were assessed using the QCL-1000® Endpoint Chromogenic LAL Assay (Lonza, Basel, Switzerland) according to the manufacturer's instructions. This measurement on high-G alginate microspheres yielded 0.000615EU/ug particles, well below levels stimulatory for innate immune cells [36-38].

Self-gelling alginate gels were formulated by pelleting calcium reservoir SLG20 microspheres (quantities as noted in the text), resuspending the particles in a minimal residual volume of water with a bath sonicator for 2 min, and adding Pronova SLM20 (0.01g/mL in PBS) alginate matrix to a constant final volume (i.e. 170 μL microspheres +alginate), dispersing microspheres throughout the solution. For delivery of self-gelling alginate *in vivo*, 150μL of microspheres/solution mixture was immediately drawn by an insulin syringe (28gauge, BD Biosciences) and injected *s.c.* in anesthetized mice.

Ca^{2+} quantification in alginate microspheres and self-gelled alginate

Alginate microspheres (100 μL of stock suspension) were pelleted and dissolved with EDTA (ethylenediaminetetraacetic acid disodium salt dehydrate; 100 μL, 2.5mM in water) and 890 μL PBS, with 10 min of sonication. Mag-fura-2 dye (5 μg/mL) was added to the dissolved microsphere solution and fluorescence was recorded on a SpectraMax M2 Microplate Reader (Molecular Devices, Sunnyvale, CA) at 340ex/515em and 380ex/515em in a flat-bottom 96-well UV-transparent plate (BD Falcon, Franklin Lakes, NJ) alongside a series of Ca^{2+} dilution standards. Calcium levels were determined using the ratio of emission intensities recorded from 340 nm and 380 nm excitation, calibrated to calcium concentration by the standard dilutions and accounting for the fraction of calcium chelated by EDTA. In parallel, some microsphere samples were dissolved with EDTA and elemental analysis was performed using inductively coupled plasma optical emission spectroscopy by Quantitative Technologies, Inc. (Whitehouse, NJ). Elemental analysis on in vitro-formed or explanted gels was performed following digestion of gels with 100 μL of 100 mM EDTA and100 μL of 10 mg/mL alginate lyase for 24 hrs at 20°C or until dissolved.

Kinetics of Ca^{2+} redistribution in self-gelling formulations

For time-lapse microscopy analysis of Ca^{2+} redistribution from microspheres into alginate solutions, 200 μL of alginate matrix solution (0.01 g/mL SLM20) pre-incubated with 25 μg/mL mag-fura-2 solution for 2 hrs was imaged in a 8-well Labtek chambered coverslip (Nalge Nunc, Rochester, NY) on a Zeiss Axiovert 200 epifluorescence microscope equipped with a CoolSnap HQ CCD camera (Princeton Instruments Inc., Acton, MA). Time-lapse fluorescence images of the samples were collected at 340 nm ex/515 nm em and 380 nm ex/515 nm em at 45 sec intervals for 10 min using a 40× objective to establish the baseline fluorescence. Microspheres (1.25×10^6) were then mixed with the matrix solution containing the dye and time-lapse recording of mag-fura fluorescence was continued for 60 min. All data was acquired and fluorescence emission ratios (340 ex:380 ex) were analyzed using Metamorph software.

Complementary Ca^{2+} redistribution measurements were made for bulk solutions using a fluorescence plate reader: calcium reservoir microspheres were mixed with matrix alginate and at staggered timepoints following mixing, microsphere/SLM20 solutions were centrifuged at 16000×g for 10 min to separate microspheres from the alginate solution. The

supernatant solution was mixed with mag-fura-2 dye (5 μg/mL) in a UV-transparent 96-well plate and fluorescence signals were acquired using a SpectraMax M2 Microplate Reader and analyzed as described above.

Shear modulus measurements

The shear moduli (G′ and G″) of self-gelled alginate gels were measured using a parallel plate configuration on an AR-G2 rheometer (TA instruments, New Castle, DE) connected to a Julabo F25 Refrigerated/Heating Circulator (Seelbach/Black Forest, Germany). Self-gelling alginate containing different amounts of SLG20 microspheres were mixed and immediately pipetted onto the bottom plate and were allowed to gel for 1 hr at 25°C. A solvent trap cover was used to prevent water loss during gelation/measurements. Oscillatory shear was then applied at an angular frequency of 1 rad/s and a controlled strain of 5% with 450μm gap, a condition that showed minimal wall slip effects. Time sweep measurements were taken for 35 min (the moduli reported are the time-averaged values), followed by frequency and strain sweeps for each sample.

Animals and cells

Animals were cared for in the USDA-inspected MIT Animal Facility under federal, state, local and NIH guidelines for animal care. C57Bl/6 mice and C57Bl/6 mice expressing green fluorescent protein (GFP) under the chicken β-actin promoter and cytomegalovirus enhancer were obtained from Jackson Laboratories. Bone marrow-derived dendritic cells (BMDCs) were prepared by isolating bone marrow from the tibias and femurs of C57Bl/6 mice or GFP+ mice and culturing them *in vitro* over 6 days in the presence of 10ng/mL GM-CSF in complete medium (RPMI 1640 containing 10% FCS, 2 mM L-Glutamine, penicillin/ streptomycin, and 50 μM 2-mercaptoethanol) following a modification of the procedure of Inaba [27] as previously reported [28]. BMDCs were used on day 6 or 7 as resting immature DCs or stimulated with CpG overnight (~18 hrs) as activated mature DCs.

IL-2 release from self-gelling alginate in vitro

Alginate particles (3×10^6) were pelleted as above, mixed with 2 μg IL-2 (100μg/mL) for 18 hrs at 4°C, and then directly added to 1% Pronova SLM20 (140 μL of 0.01g/mL in PBS) matrix to form a gel. All samples were allowed to gel at 37°C for 2 hrs while gently shaking, followed by a gentle wash with 1 mL of complete medium. Release studies were conducted by adding 1mL of the complete medium to gels at 37°C; 950 μL of supernatant was removed at each time point over 7 days and fresh medium added to replace that withdrawn. The supernatants were stored at 4°C until all the time points were collected, and on day 7 the alginate gels were digested with 10mg/mL alginate lyase for ~20 min at 37°C to recover all remaining cytokine. The amounts of cytokine in supernatants from each sample were quantified by sandwich ELISA according to the manufacturer's instructions (R&D Systems, Minneapolis, MN). The bioactivity of IL-2 released from alginate was tested by measuring proliferation induced in the IL-2-dependent cell line CTLL-2 (generously provided by Laboratory of Prof. Dane Wittrup at MIT) compared to solution standards of IL-2, using the WST-1 proliferation assay (Roche Applied Science, Mannheim, Germany) according to the manufacturer's instructions.

CpG/Poly-L-Lysine-coated alginate particles and BMDC stimulation

Alginate microspheres synthesized under sterile conditions were incubated with 2 mg/mL poly-L-lysine in sterile DD H_2O for 2 hr at 20°C while rotating with a Labquake rotator, washed 3× with 1 mL of sterile DD H_2O, followed by incubation with 50 μM CpG or FITC-CpG (in PBS) solution (5 nmoles CpG/FITC-CpG per 10^6 particles) overnight at 4°C while

rotating. The microspheres were washed $3\times$ again with sterile DD H_2O and resuspended at a concentration of 10×10^6 particles/mL.

Microspheres (10^6 or 0.5×10^6 unmodified, Poly-L-lysine coated, or CpG/PLL-coated) or control soluble CpG were added to day-5 BMDC cultures containing 10^6 cells/mL and incubated at 37°C for 18 hrs. Treated or control BMDCs were harvested from culture plates, blocked with 10 μg/mL anti-CD16/CD32 antibody for 10 min at 4°C, and stained with fluorescent antibodies against surface markers (CD11c, I-A[b], and CD40) for 20 min on ice. Stained cells were analyzed on a BD FACSCalibur flow cytometer (BD Biosciences).

FITC-CpG release from FITC-CpG/PLL alginate microspheres

FITC-CpG/PLL-coated alginate microspheres were prepared as described above, and 10^6 particles were either aliquotted into Eppendorf tubes by themselves or encapsulated into self-gelled alginate (140 μL 0.01 g/mL SLM20 in PBS + 3×10^6 calcium reservoir microspheres) containing 11 mM calcium. Samples were washed once with 1 mL of phenol-red free RPMI 1640 with 10% FCS. Release measurements were initiated by adding 300 μL of complete medium (phenol-red free); at each timepoint the supernatant was collected and 300 μL fresh medium added to the samples over a 7-day period. The amount of FITC-CpG released into the media was quantified by the intensity of FITC fluorescence in the supernatant using a Perkin-Elmer HTS 7000 Plus Bio Assay Reader (Waltham, MA) with 492 nm ex and 535 nm em, calibrated by a serial dilution of FITC-CpG standard solutions.

Fluorescence and reflectance-mode confocal microscopy

For *in vitro* samples, SLM20 alginate labeled with 6-aminofluorescein (130μL of 0.01g/mL in PBS) was mixed with 4×10^6 calcium reservoir microspheres (~14.8mM Ca^{2+}). For injected gels, C57Bl/6 BMDCs (2×10^6) were washed $3\times$ with PBS and mixed with 160 μL fluorescently-labeled SLM20 (0.01 g/mL in PBS) and 10^6 calcium-reservoir microspheres, then 150μL of the alginate/cell suspension was injected *s.c.* into the flanks of anesthetized C57Bl/6 or GFP[+] mice with a 28 gauge insulin syringe (BD Biosciences). Animals were euthanized and gels were explanted from mice 22-48 hrs after inoculation and imaged using a Zeiss LSM 510 confocal microscope (Thornwood, NY). Reflectance mode imaging was obtained by collecting back-scattered light using a 488nm laser for illumination. 3D reconstructed images were obtained through 100-300 μm depths in 1-2 μm *z*-steps using a 40× water-immersion objective. 3D reconstruction and projections over multiple *z*-planes were processed using Volocity software (Improvision Inc, Waltham, MA).

Results and Discussion

Characterization of calcium-reservoir microspheres

Prior studies have demonstrated that alginate microspheres of sizes 1-250 μm diameter can be prepared using water-in-oil emulsions [29,30]. Similarly, we synthesized calcium-loaded alginate microspheres by emulsification of an aq. solution of alginate in isooctane containing surfactants, followed by crosslinking of alginate droplets via addition of aq. calcium to the emulsion (Figure 1). In order to form microsphere reservoirs that could bind substantial amounts of calcium, particles were formed from high-G alginate (Pronova SLG20, >60% G unit), based on the higher affinity of G units of alginate for calcium compared to M units [6,31,32]. Each synthesis produced ~10×10^6 calcium reservoir microspheres (CRMs) and the resulting microspheres had mean diameters of 12 μm ± 9 μm with a pellet volume of ~10 μL per 10^6 microspheres. Calcium loading was measured by dissolving the microspheres with EDTA and PBS, followed by measurement of released ions using the calcium-sensitive fluorescent dye mag-fura-2 [33-35]. Using this technique, the microspheres were found to contain an average of 1.5 ± 0.2 μmol of Ca^{2+} per mg alginate (*n*

> 10 independent batches of particles). Elemental analysis of these samples yielded an average of 1.6 ± 0.2 μmoles of Ca^{2+} (n=6), consistent with the fluorescence assay. The microspheres exhibited no swelling over the course of a week and were stable for at least 7 days in water. Analysis of the supernatant from CRM suspensions using mag-fura-2 indicated that the concentration of free Ca^{2+} in the supernatant was effectively zero and little Ca^{2+} was released into the aqueous phase during storage.

Gelation of alginate solutions using calcium-reservoir microspheres

The concept of self-gelling alginate using calcium-loaded microspheres is illustrated in Figure 1. Upon mixing of alginate microspheres with an alginate aqueous solution in PBS, calcium ions rapidly diffused from the microspheres into the solution to form a stable alginate gel, facilitated by sodium ion exchange. Alginate with a high M content (Pronova SLM20, >50% M units), which forms a mechanically less rigid gel than G-rich alginate [11,31,39], was used as the solution matrix component to favor cell infiltration into gels in their ultimate *in vivo* application. To measure the kinetics of calcium redistribution upon mixing CRMs with matrix alginate for self-gelation, we used the same microsphere/matrix composition applied for *in vivo* injections described later (9×10^5 CRMs mixed with 150μL SLM20 alginate (0.01 g/mL in PBS)). As described below, this composition does not form a stable gel *in vitro* but forms a low-viscosity alginate solution (additional calcium from the surrounding tissues contributes in *vivo*); we used this sub-gelation condition as a strategy to allow calcium redistribution followed by rapid separation of microspheres from the still-fluid alginate matrix solution (via centrifugation), in order to measure the amount of calcium released into the matrix solution. First, calcium redistribution kinetics was characterized using a calcium-sensitive dye, mag-fura-2, tracking the ratio of fluorescence emission following excitation at wavelengths of 340 nm vs. 380 nm over time by time-lapse fluorescence microscopy. Figure 2A shows a representative temporal trace of calcium levels detected in the alginate solution by mag-fura-2 following addition of CRMs, illustrating the extremely rapid release of calcium into the PBS/alginate matrix. Taking into account the physical act of mixing (~3 min), the microspheres released Ca^{2+} within the first several min of mixing of the particles with the matrix solution. Bulk fluorescence measurements on a fluorescent plate reader following separation of microspheres from the matrix alginate after 12 min showed 2.3-2.6 mM Ca^{2+} in the alginate solution (data not shown), consistent with the data from time-lapse microscopy, a concentration that was constant for up to 1 week. Since the total calcium concentration in the alginate matrix + microspheres (as determined by elemental analysis) was 3.7 ± 0.3 mM for this composition, approximately 70% of calcium initially present in the CRMs was released within the first few minutes, and the remaining calcium remained sequestered within the particles for at least 7 days. Consistent with the rapid ion redistribution kinetics measured by the calcium-sensitive dye reporter, when fluorescent polystyrene nanoparticles (500 nm diam.) were mixed with self-gelling alginate containing a greater total content of calcium by adding 4-fold more CRMs to alginate matrix solutions (14.8 mM total calcium), time-lapse fluorescence imaging showed a cessation of nanoparticle Brownian motion within 5 min, indicating gelation on short timescales when sufficient calcium-reservoir microspheres were present (data not shown). This data is also consistent with a prior study, which reported an increase of the shear elastic modulus of alginate within the first several minutes of mixing of alginate with alginate-associated calcium [17].

The microscale structure of self-gelled alginate was visualized by employing fluorescein-labeled SLM20 as the matrix mixed with unlabeled SLG20 microspheres (net calcium concentration ~14.8 mM). Examination of the structures of the resulting gels by confocal microscopy showed a random distribution of the polydisperse calcium-reservoir

microspheres (indicated by the non-fluorescent spherical voids) throughout the alginate matrix (Figure 2B).

Mechanical properties of self-gelled alginate hydrogels

Because the concentration of CRMs directly determines the amount of calcium in self-gelling formulation, the mechanical properties of the resulting gels were directly modulated by the amounts of particles added. Figure 3A shows the shear moduli of self-gelled alginate containing different amounts of SLG20 microspheres, as measured by parallel plate rheometer. Each gel composition was allowed to set on the rheometer plate for 1 hr at 25°C before small oscillatory shear was applied. Figure 3B shows the shear modulus over a range of angular frequencies for gels with ~8.6mM calcium concentration, showing the dominance of elastic behavior over two decades of angular frequency. Similar behavior was seen for gels with calcium concentrations above ~6mM (data not shown). The amplitude of the strain (5%) used for all the measurements fell within the linear region of the viscoelastic spectrum as shown in Figure 3C (for the case of ~8.6mM calcium concentration). Prior studies have generally reported elastic moduli measured for gels containing substantially higher calcium concentrations (> 50-100 mM) and are on the order of 10^3 Pa [40-43]. However, direct comparison is difficult since the mechanical properties of alginate are affected by the alginate block structure, molecular weight, G/M ratio, and concentration. The mechanical properties are also dependent on the electrolyte composition of the gelling medium, since monovalent ions will compete for binding sites despite the high affinity of calcium ions with alginate G units[44]. Such a mechanism is clearly involved in the present case where the matrix alginate was in PBS solution (0.14M NaCl, 3mM KCl, 10mM K_2HPO_4, pH=7.4), leading to mechanically soft gels as observed by LeRoux et al. for alginate gelled in the presence of 0.15M NaCl [45], and as Khromova observed for alginate gelled in the presence of KCl [15].

Ionically crosslinked alginate is easily displaced from equilibrium by mechanical forces, and its behavior is heavily influenced by kinetics despite its elastic behavior at low strains [44]. In addition, alginate is a shear-thinning fluid [31]. Thus, even for matrix/microsphere mixtures providing > 6 mM total Ca^{2+}, gels with constant and stable shear moduli were not achievable when shear was applied immediately after loading onto the rheometer stage (data not shown); precluding measurement of the change in shear modulus with time. However, this behavior facilitated mixing of the matrix solution and microspheres; despite rapid ion release, uniform mixing of the calcium-loaded microspheres and the matrix was feasible even at relatively high CRM concentrations because application of shear during mixing disrupted crosslinking. The self-gelling system is thus suitable for applications in which mechanically soft yet uniform and stable gels are desired.

Sustained release of IL-2 from self-gelling alginate

Due to its mild gelation conditions, alginate has become an attractive candidate for encapsulation and delivery of proteins and other drugs in recent years [19,46-49]. We are particularly interested in the application of self-gelling alginate for co-delivery of immune cells and immunoregulatory factors at tumor sites to promote anti-tumor immune responses. We previously demonstrated that dendritic cells (DCs) are readily encapsulated in subcutaneously-injected self-gelling alginate [19], and in order to augment their functions, we sought to co-deliver immunoregulatory factors in these gels that could play complementary roles in supporting anti-tumor immune responses: the immunocytokine interleukin-2 (IL-2) and CpG oligonucleotides. To build on the self-gelling system already described, we encapsulated IL-2 into the gels, and used alginate microspheres as modular components to immobilize CpG on their surfaces and mix them along with CRMs into matrix alginate solutions (Figure 1).

IL-2 is a cytokine that supports proliferation and effector functions of lymphocytes[50-54]. It is FDA-approved for treatment of metastatic melanoma and renal cell carcinoma via systemic injection, but is known to have dose-limiting toxicity. Thus, strategies for local delivery at tumor sites have been sought to maximize the effectiveness of this cytokine: Slow release of IL-2 has been previously demonstrated using controlled release polymers [55-57], including alginate [58]. For IL-2 delivery in this self-gelling system, we mixed 2 μg of murine IL-2 with CRMs and matrix alginate solution for gelation (3×10^6 microspheres/ 140μL alginate matrix solution, giving ~11mM Ca^{2+}). Release of IL-2 from the resulting gels was measured by ELISA analysis of gel supernatants over 7 days. As shown in Figure 4, the self-gelling alginate released IL-2 in a sustained manner over a week *in vitro*, suggesting that cytokines can be co-delivered from these gels into the surrounding microenvironment for a prolonged period following injection. The bioactivity of IL-2 released from these gels (assessed using the IL-2-dependent cell line CTLL-2) was statistically indistinguishable (95% bioactive) from control IL-2 solutions (data not shown). We have previously shown that highly cationic proteins exhibit very slow release from alginate gels due to electrostatic interactions with the matrix, but IL-2 has an isoelectric point near neutral pH. Thus, similar to the conclusions of other studies of cytokine release from alginate-based gels [58] [59], we speculate that the release kinetics are mediated primarily via diffusion of IL-2 through the molecular mesh of the alginate gel.

Functionalization of alginate microspheres with CpG oligonucleotides

In addition to providing IL-2 locally to recruited T-cells, we sought a strategy to provide activation signals locally to host DCs attracted to injectable alginate gels. CpG oligonucleotides, short single-stranded DNA oligos that mimic bacterial DNA strands and activate dendritic cells via Toll-like receptor-9, have been shown to potently activate DCs in cancer settings and to break tolerance to tumor antigens [60-64]. Thus, we tested an approach to immobilize CpG oligos electrostatically on the surface of alginate microspheres for incorporation into self-gelling alginate formulations (Figure 1): the polycation poly-L-lysine (PLL) was adsorbed to the anionic surfaces of CRMs followed by electrostatic adsorption of CpG oligos (unlabeled or FITC-tagged CpG) to the PLL-modified alginate particles. Fluorescence micrographs of FITC-CpG/PLL/alginate particles (Figure 5A) showed clear binding of FITC-CpG to PLL-modified microspheres, and fluorescence measurements showed that ~88% of the FITC-CpG added (5 nmol FITC-CpG incubated with 10^6 particles) bound to PLL-coated microspheres. To assess the stability of CpG binding to PLL/alginate particles, we measured the release of fluorescent CpG into supernatants of CpG/PLL/alginate particle suspensions, self-gelled alginate containing the same number of CpG/PLL/alginate particles, or self-gelled alginate encapsulating equivalent amounts of soluble CpG (not immobilized). As shown in Figure 5B, most soluble FITC-CpG was released from self-gelling alginate by ~5 days, whereas release of CpG bound to particles was substantially slower, with only ~20% released over 1 week from either the particles alone or from the particles encapsulated in self-gelling alginate.

In order to test whether CpG bound to alginate particles was capable of eliciting DC activation, bone-marrow derived dendritic cells (BMDCs) were incubated with CpG/PLL/ alginate particles, PLL/alginate particles, alginate particles, or soluble CpG as a positive control for 18 hrs. Figure 5C shows flow cytometry scatter plots gated on CD11c+ cells for each condition: While almost no untreated control BMDCs have a highly mature (activated) MHC IIhiCD40hi phenotype, ~20% of soluble CpG-stimulated DCs show this phenotype by 18 hrs. BMDCs co-cultured with alginate or PLL/alginate microspheres showed similar phenotypes as untreated immature DCs, whereas the CpG-coated particles caused upregulation of the CD40 and MHC class II molecules on the DCs comparable to the soluble CpG positive control. The viability of the cells, as assessed by PI (propidium iodide)

staining, did not differ among the conditions tested, indicating no cytotoxicity of the unmodified, PLL-coated, or CpG/PLL-coated alginate microspheres (data not shown). In addition to upregulation of these molecules involved in T-cell priming, another key function of activated DCs is the production of proinflammatory cytokines. Figures 5D and E show that the CpG/PLL-coated microspheres triggered secretion of the pro-inflammatory cytokines IL-6 and IL-12p70 by BMDCs at least as efficiently as soluble CpG. Taken together, the above data suggests that alginate microspheres do not themselves activate dendritic cells, consistent with published data [65], but CpG oligonucleotides can be immobilized to these particles with slow release over periods in excess of 1 week, and CpG-modified CRMs mediate potent activation of DCs.

Gel structure and cellular infiltration of self-gelling alginate in vivo

In order to formulate a composition of CRMs and alginate matrix suitable for injection *in vivo*, a series of compositions were tested for their ability to be readily drawn into and ejected from an insulin syringe (28 gauge). Based on this practical requirement, a composition with 6×10^3 CRMs/ μL SLM20 solution was selected for testing *in vivo* (overall calcium concentration of 3.7 ± 0.3 mM). Though the amount of crosslinking ions provided by the CRMs in this formulation gives weak mechanical properties *in vitro* (Figure 3), we hypothesized that calcium available in the interstitial fluid would contribute to crosslinking *in vivo*. Indeed, as shown in Table 1, when this formulation was injected *in vivo* subcutaneously in C57Bl/6 mice and explanted after 2 hrs, ~8 mM Ca^{2+} was detected in the recovered gels by elemental analysis, corresponding to gels with elastic behavior over a range of oscillatory frequencies (Figures 3A and B), and a Ca^{2+} contribution from the interstitial fluid of ~4.5 mM. When alginate precursor solution was injected without added CRMs and explanted after 2 hrs, 5.5 mM calcium was detected by elemental analysis, corresponding to gels with ~60-fold lower shear moduli. Thus, formulations with low concentrations of CRMs that are unable to themselves form stable gels facilitate preparation of solutions/handling, while achieving soft but stable gels following injection *in vivo* via the contribution of extracellular calcium in the tissue.

Gels formed *in vitro* in the studies described in previous sections form under idealized conditions of pure buffer solutions, in the absence of serum or blood factors that are present *in vivo*. To determine the structure of gels formed following *in vivo* injection, we injected self-gelling alginate (6×10^3 CRMs/μL SLM20 solution) *s.c.* in C57Bl/6 mice, explanted the resulting gels 22-48 hrs after injection, and examined them in their native, hydrated state by 3D confocal microscopy. We first examined the explanted gels by reflectance-mode confocal microscopy, a technique to visualize the surface and volume architecture and topology of three-dimensional matrices including natural biopolymers such as collagen [66,67] as well as synthetic polymer matrices [68]. Nano-scale fibrils of extracellular matrix (ECM) can be resolved *in situ* through this method without the need for exogenous labeling [67]. Figure 6A shows representative brightfield and reflectance-mode images of a self-gelled alginate matrix explanted 19 hrs after injection, showing fibrillar structures that are of micron scale. Such fibrillar structures were readily resolved within explanted alginate gels up to *z*-depths as far as reflectance could resolve (~100 μm). In contrast, self-gelled alginate matrices formed *in vitro* were generally featureless in reflectance microscopy (data not shown). To determine whether these fibrillar structures represented a morphological change induced by alginate itself *in vivo* or were instead exogenous like ECM components or blood factors such as fibrin depositing in the gels, fluorescent alginate was injected, and we examined the structure in regions where fibrillar structures were prominent enough to be observed directly in brightfield images. Figure 6B illustrates that fibrillar structures formed within these gels (observed in brightfield) were not associated with alginate chains (green fluorescence) but actually occupied voidspaces in the gels where alginate was absent,

demonstrating that the self-gelling alginate forms a macroporous structure *in vivo*, possibly intertwined with as yet-undefined ECM components present in the serum, the interstitial fluid, and/or the blood.

To determine whether CpG-coated microspheres could maintain local depots of CpG within these gels *in vivo*, we injected self-gelling alginate carrying Cy5-labeled-CpG/PLL-coated alginate microspheres, non-coated CRMs, and activated, unlabeled BMDCs into transgenic GFP+ mice. Gels were explanted after 24 or 48 hrs and analyzed by 3D confocal microscopy. Figure 6C shows that the Cy5-CpG-coated microspheres remained intact for at least 48 hrs *in vivo* (left panel). Host cells (green) were also observed clustering around CpG-bearing microspheres (Figure 6C right panel), and ingesting fluorescent CpG (Figure 6C left and right panels). We have previously shown that a large number of host DCs infiltrate alginate gels loaded with exogenous (syngeneic) activated DCs, within 48 hrs post injection [19]. Availability of CpG on the surface of alginate microspheres for a prolonged time period might thus enable sustained local activation of recruited host DCs within the matrix.

The success of a synthetic tissue engineering scaffold as a replacement for the native tissue environment depends, among other factors, on its three-dimensional micro-architecture and mechanical integrity, and ability to support cellular migration/infiltration [32,69]. In order to visualize how host cells invade injected alginate matricesself-gelling alginate labeled with a far-red dye, Hilyte Fluor 647, and containing activated, unlabeled BMDCs was injected into transgenic GFP+ mice. Fluorescence confocal microscopy of explanted gels at 48 hrs revealed that host cells from the surrounding tissue invade the matrix via potentially two means (Figure 7): cells occupied void spaces in the macroporous gel structure and extended lamellipodia into void spaces (blue arrows), suggesting they preferentially infiltrated pre-existing pores. In addition, phagocytic cells were also observed with intracellular deposits of alginate (clearly intracellular when observed in reconstructed *z*-sections, not shown), indicating ingestion of alginate by some cells as they infiltrated and made their own way through the matrix. Examination of cell migration inside the gels under time-lapse microscopy also revealed smaller cells rapidly migrating by squeezing through small void spaces. This observation is consistent with the recent studies demonstrating that leukocytes can rapidly migrate through porous matrices in the total absence of functional integrins [70]. Thus, cellular infiltration is supported by the macroporosity of *in situ*-gelled alginate, and potentially by ECM molecules deposited within the gel during injection.

Conclusions

We analyzed the physical properties of self-gelling formulations of alginate formed by mixing calcium reservoir alginate microspheres with a soluble alginate solution. We found that relatively stable gels were formed for matrices loaded with $>\sim 6$ mM Ca^{2+}, whether provided by microspheres only *in vitro*, or by a combination of ions from the reservoir microspheres and surrounding tissue fluid *in vivo*. Redistribution of calcium ions from the reservoir microspheres was rapid, reaching equilibrium within minutes of mixing with alginate aqueous solutions. Cellular infiltration of these gels is supported by the macroporous morphology of gels formed i*n situ* following injection. This alginate microsphere + alginate solution strategy for forming gels allows injectable formulations to be achieved without introducing additional compounds or components to the system (the final matrix contains only alginate). In addition, the microspheres can serve a dual function as both reservoirs for calcium and as microdepots for presentation or release of co-factors in the matrix. The ability to incorporate soluble factors like IL-2 directly into matrix and to use microspheres as modular components for augmenting these gels with slowly released factors, such as CpG oligonucleotides as demonstrated here, may provide a potent platform

for immunotherapy when combined with delivery of immune cells. In addition, such non-invasively delivered gels may be of general interest for tissue engineering and regenerative medicine applications.

Acknowledgments

References

1. Chang SC, et al. Injection molding of chondrocyte/alginate constructs in the shape of facial implants. J Biomed Mater Res 2001;55(4):503–11. [PubMed: 11288078]

2. Cirone P, Bourgeois JM, Austin RC, Chang PL. A novel approach to tumor suppression with microencapsulated recombinant cells. Hum Gene Ther 2002;13(10):1157–66. [PubMed: 12133269]

3. Joki T, et al. Continuous release of endostatin from microencapsulated engineered cells for tumor therapy. Nat Biotechnol 2001;19(1):35–9. [PubMed: 11135549]

4. Shang Q, Wang Z, Liu W, Shi Y, Cui L, Cao Y. Tissue-engineered bone repair of sheep cranial defects with autologous bone marrow stromal cells. J Craniofac Surg 2001;12(6):586–93. discussion 594-5. [PubMed: 11711828]

5. Thomas S. Alginate dressings in surgery and wound management--Part 1. J Wound Care 2000;9(2): 56–60. [PubMed: 11933281]

6. Sikorski P, Mo F, Skjak-Braek G, Stokke BT. Evidence for egg-box-compatible interactions in calcium-alginate gels from fiber X-ray diffraction. Biomacromolecules 2007;8(7):2098–103. [PubMed: 17530892]

7. Boontheekul T, Kong HJ, Mooney DJ. Controlling alginate gel degradation utilizing partial oxidation and bimodal molecular weight distribution. Biomaterials 2005;26(15):2455–65. [PubMed: 15585248]

8. Kong HJ, Kaigler D, Kim K, Mooney DJ. Controlling rigidity and degradation of alginate hydrogels via molecular weight distribution. Biomacromolecules 2004;5(5):1720–7. [PubMed: 15360280]

9. Gomez CG, Rinaudo M, Villar MA. Oxidation of sodium alginate and characterization of the oxidized derivatives. Carbohydrate Polymers 2006;67(3):296–304.

10. Wang T, et al. An encapsulation system for the immunoisolation of pancreatic islets. Nat Biotechnol 1997;15(4):358–62. [PubMed: 9094138]

11. Kuo CK, Ma PX. Ionically crosslinked alginate hydrogels as scaffolds for tissue engineering: part 1. Structure, gelation rate and mechanical properties. Biomaterials 2001;22(6):511–21. [PubMed: 11219714]

12. Marler JJ, et al. Soft-tissue augmentation with injectable alginate and syngeneic fibroblasts. Plast Reconstr Surg 2000;105(6):2049–58. [PubMed: 10839402]

13. Rowley JA, Mooney DJ. Alginate type and RGD density control myoblast phenotype. J Biomed Mater Res 2002;60(2):217–23. [PubMed: 11857427]

14. Poncelet D, Poncelet De Smet B, Beaulieu C, Huguet ML, Fournier A, Neufeld RJ. production of alginate beads by emulsification/internal gelation. II. Physicochemistry. Applied Microbiology and Biotechnology 1995;43:644–650.

15. Khromova YL. The Effect of Chlorides on Alginate Gelation in the Presence of Calcium Sulfate. Kolloidnyi Zhurnal 2006;68(1):123–128.

16. Reis CP, Neufeld RJ, Vilela S, Ribeiro AJ, Veiga F. Review and current status of emulsion/dispersion technology using an internal gelation process for the design of alginate particles. J Microencapsul 2006;23(3):245–57. [PubMed: 16801237]

17. Melvik, JE.; D, M.; Onsoyen, E.; Berge, A.; Svendsen, T. Self-gelling alginate systems and uses thereof patent. United States Patent Application #20060159823. 2006. inventor

18. Westhaus E, Messersmith PB. Triggered release of calcium from lipid vesicles: a bioinspired strategy for rapid gelation of polysaccharide and protein hydrogels. Biomaterials 2001;22(5):453–62. [PubMed: 11214756]

19. Hori Y, Winans AM, Huang CC, Horrigan EM, Irvine DJ. Injectable dendritic cell-carrying alginate gels for immunization and immunotherapy. Biomaterials. 2008

20. Banchereau J, et al. Immunobiology of dendritic cells. Annu Rev Immunol 2000;18:767–811. [PubMed: 10837075]

21. Gilboa E. DC-based cancer vaccines. J Clin Invest 2007;117(5):1195–203. [PubMed: 17476349]

22. Lu W, Wu X, Lu Y, Guo W, Andrieu JM. Therapeutic dendritic-cell vaccine for simian AIDS. Nat Med 2003;9(1):27–32. [PubMed: 12496959]

23. Nestle FO, Farkas A, Conrad C. Dendritic-cell-based therapeutic vaccination against cancer. Curr Opin Immunol 2005;17(2):163–9. [PubMed: 15766676]

24. Steinman RM, Banchereau J. Taking dendritic cells into medicine. Nature 2007;449(7161):419–26. [PubMed: 17898760]

25. Timmerman JM, Levy R. Dendritic cell vaccines for cancer immunotherapy. Annu Rev Med 1999;50:507–29. [PubMed: 10073291]

26. Landa N, et al. Effect of injectable alginate implant on cardiac remodeling and function after recent and old infarcts in rat. Circulation 2008;117(11):1388–96. [PubMed: 18316487]

27. Inaba K, et al. Generation of large numbers of dendritic cells from mouse bone marrow cultures supplemented with granulocyte/macrophage colony-stimulating factor. J Exp Med 1992;176(6): 1693–702. [PubMed: 1460426]

28. Stachowiak AN, Wang Y, Huang YC, Irvine DJ. Homeostatic lymphoid chemokines synergize with adhesion ligands to trigger T and B lymphocyte chemokinesis. J Immunol 2006;177(4):2340–8. [PubMed: 16887995]

29. Ghiasi Z, Sajadi Tabasi SA, Tafaghodi M. Preparation and *In Vitro* Characterization of Alginate Microspheres Encapsulated with Autoclaved *Leishmania major* (ALM) and CpG-ODN. Iranian Journal of Basic Medical Sciences 2007;10(2):90–98.

30. Lee HY, Chan LW, Heng PW. Influence of partially cross-linked alginate used in the production of alginate microspheres by emulsification. J Microencapsul 2005;22(3):275–80. [PubMed: 16019913]

31. Augst AD, Kong HJ, Mooney DJ. Alginate hydrogels as biomaterials. Macromol Biosci 2006;6(8): 623–33. [PubMed: 16881042]

32. Rowley JA, Madlambayan G, Mooney DJ. Alginate hydrogels as synthetic extracellular matrix materials. Biomaterials 1999;20(1):45–53. [PubMed: 9916770]

33. Hofer AM, Machen TE. Technique for in situ measurement of calcium in intracellular inositol 1,4,5-trisphosphate-sensitive stores using the fluorescent indicator mag-fura-2. Proc Natl Acad Sci U S A 1993;90(7):2598–602. [PubMed: 8464866]

34. Raju B, Murphy E, Levy LA, Hall RD, London RE. A fluorescent indicator for measuring cytosolic free magnesium. Am J Physiol 1989;256(3 Pt 1):C540–8. [PubMed: 2923192]

35. Tsien RY. Fluorescent probes of cell signaling. Annu Rev Neurosci 1989;12:227–53. [PubMed: 2648950]

36. Hu Y, et al. Cytosolic delivery of membrane-impermeable molecules in dendritic cells using pH-responsive core-shell nanoparticles. Nano Lett 2007;7(10):3056–64. [PubMed: 17887715]

37. Jotwani R, Pulendran B, Agrawal S, Cutler CW. Human dendritic cells respond to Porphyromonas gingivalis LPS by promoting a Th2 effector response in vitro. Eur J Immunol 2003;33(11):2980–6. [PubMed: 14579266]

38. Vallhov H, et al. The importance of an endotoxin-free environment during the production of nanoparticles used in medical applications. Nano Lett 2006;6(8):1682–6. [PubMed: 16895356]

39. Smidsrod O, Skjak-Braek G. Alginate as immobilization matrix for cells. Trends Biotechnol 1990;8(3):71–8. [PubMed: 1366500]

40. Kong HJ, Smith MK, Mooney DJ. Designing alginate hydrogels to maintain viability of immobilized cells. Biomaterials 2003;24(22):4023–9. [PubMed: 12834597]

41. Kong HJ, Wong E, Mooney DJ. Independent Control of Rigidity and Toughness of Polymeric Hydrogels. Macromolecules 2003;36:4582–4588.

42. Ahearne M, Yang Y, El Haj AJ, Then KY, Liu KK. Characterizing the viscoelastic properties of thin hydrogel-based constructs for tissue engineering applications. J R Soc Interface 2005;2(5): 455–63. [PubMed: 16849205]

43. West ER, Xu M, Woodruff TK, Shea LD. Physical properties of alginate hydrogels and their effects on in vitro follicle development. Biomaterials 2007;28(30):4439–48. [PubMed: 17643486]

44. Webber RE, Shull KR. Strain Dependence of the Viscoelastic Properties of Alginate Hydrogels. Macromolecules 2004;37:6153–6160.

45. LeRoux MA, Guilak F, Setton LA. Compressive and shear properties of alginate gel: effects of sodium ions and alginate concentration. J Biomed Mater Res 1999;47(1):46–53. [PubMed: 10400879]

46. Freeman I, Kedem A, Cohen S. The effect of sulfation of alginate hydrogels on the specific binding and controlled release of heparin-binding proteins. Biomaterials 2008;29(22):3260–8. [PubMed: 18462788]

47. Murata Y, Jinno D, Liu D, Isobe T, Kofuji K, Kawashima S. The drug release profile from calcium-induced alginate gel beads coated with an alginate hydrolysate. Molecules 2007;12(11): 2559–66. [PubMed: 18065958]

48. Wee S, Gombotz WR. Protein release from alginate matrices. Adv Drug Deliv Rev 1998;31(3): 267–285. [PubMed: 10837629]

49. Gu F, Amsden B, Neufeld R. Sustained delivery of vascular endothelial growth factor with alginate beads. J Control Release 2004;96(3):463–72. [PubMed: 15120902]

50. Belldegrun A, Muul LM, Rosenberg SA. Interleukin 2 expanded tumor-infiltrating lymphocytes in human renal cell cancer: isolation, characterization, and antitumor activity. Cancer Res 1988;48(1):206–14. [PubMed: 3257161]

51. Kawakami Y, et al. Identification of a human melanoma antigen recognized by tumor-infiltrating lymphocytes associated with in vivo tumor rejection. Proc Natl Acad Sci U S A 1994;91(14): 6458–62. [PubMed: 8022805]

52. Topalian SL, Solomon D, Rosenberg SA. Tumor-specific cytolysis by lymphocytes infiltrating human melanomas. J Immunol 1989;142(10):3714–25. [PubMed: 2785562]

53. Wallace PK, et al. Mechanisms of adoptive immunotherapy: improved methods for in vivo tracking of tumor-infiltrating lymphocytes and lymphokine-activated killer cells. Cancer Res 1993;53(10 Suppl):2358–67. [PubMed: 8485722]

54. Rosenberg SA, Yang JC, Restifo NP. Cancer immunotherapy: moving beyond current vaccines. Nat Med 2004;10(9):909–15. [PubMed: 15340416]

55. Hanes J, et al. Controlled local delivery of interleukin-2 by biodegradable polymers protects animals from experimental brain tumors and liver tumors. Pharm Res 2001;18(7):899–906. [PubMed: 11496947]

56. Bos GW, et al. In situ crosslinked biodegradable hydrogels loaded with IL-2 are effective tools for local IL-2 therapy. Eur J Pharm Sci 2004;21(4):561–7. [PubMed: 14998588]

57. De Groot CJ, Cadee JE, Koten JE, Hennink WE, Otter WD. Therapeutic efficacy of IL-2-loaded hydrogels in a mouse tumor model. International Journal of Cancer 2002;98:134–140.

58. Liu L, Liu S, Ng SY, Froix M, Ohno T, Heller J. Controlled release of interleukin-2 for tumour immunotherapy using alginate/chitosan porous microspheres. Journal of Controlled Release 1997;43:65–74.

59. Liu XD, et al. Characterization of structure and diffusion behaviour of Ca-alginate beads prepared with external or internal calcium sources. J Microencapsul 2002;19(6):775–82. [PubMed: 12569026]

60. Kunikata N, et al. Peritumoral CpG oligodeoxynucleotide treatment inhibits tumor growth and metastasis of B16F10 melanoma cells. J Invest Dermatol 2004;123(2):395–402. [PubMed: 15245441]

61. Tokunaga T, et al. Antitumor activity of deoxyribonucleic acid fraction from Mycobacterium bovis BCG. I. Isolation, physicochemical characterization, and antitumor activity. J Natl Cancer Inst 1984;72(4):955–62. [PubMed: 6200641]

62. Vicari AP, et al. Reversal of tumor-induced dendritic cell paralysis by CpG immunostimulatory oligonucleotide and anti-interleukin 10 receptor antibody. J Exp Med 2002;196(4):541–9. [PubMed: 12186845]

63. Yang Y, Huang CT, Huang X, Pardoll DM. Persistent Toll-like receptor signals are required for reversal of regulatory T cell-mediated CD8 tolerance. Nat Immunol 2004;5(5):508–15. [PubMed: 15064759]

64. Furumoto K, Soares L, Engleman EG, Merad M. Induction of potent antitumor immunity by in situ targeting of intratumoral DCs. J Clin Invest 2004;113(5):774–83. [PubMed: 14991076]

65. Babensee JE, Paranjpe A. Differential levels of dendritic cell maturation on different biomaterials used in combination products. J Biomed Mater Res A 2005;74(4):503–10. [PubMed: 16158496]

66. Friedl P, Maaser K, Klein CE, Niggemann B, Krohne G, Zanker KS. Migration of highly aggressive MV3 melanoma cells in 3-dimensional collagen lattices results in local matrix reorganization and shedding of alpha2 and beta1 integrins and CD44. Cancer Res 1997;57(10): 2061–70. [PubMed: 9158006]

67. Brightman AO, Rajwa BP, Sturgis JE, McCallister ME, Robinson JP, Voytik-Harbin SL. Time-lapse confocal reflection microscopy of collagen fibrillogenesis and extracellular matrix assembly in vitro. Biopolymers 2000;54(3):222–34. [PubMed: 10861383]

68. Semler EJ, Tjia JS, Moghe PV. Analysis of surface microtopography of biodegradable polymer matrices using confocal reflection microscopy. Biotechnol Prog 1997;13(5):630–4. [PubMed: 9336982]

69. Griffith LG, Swartz MA. Capturing complex 3D tissue physiology in vitro. Nat Rev Mol Cell Biol 2006;7(3):211–24. [PubMed: 16496023]

70. Lammermann T, et al. Rapid leukocyte migration by integrin-independent flowing and squeezing. Nature 2008;453(7191):51–5. [PubMed: 18451854]
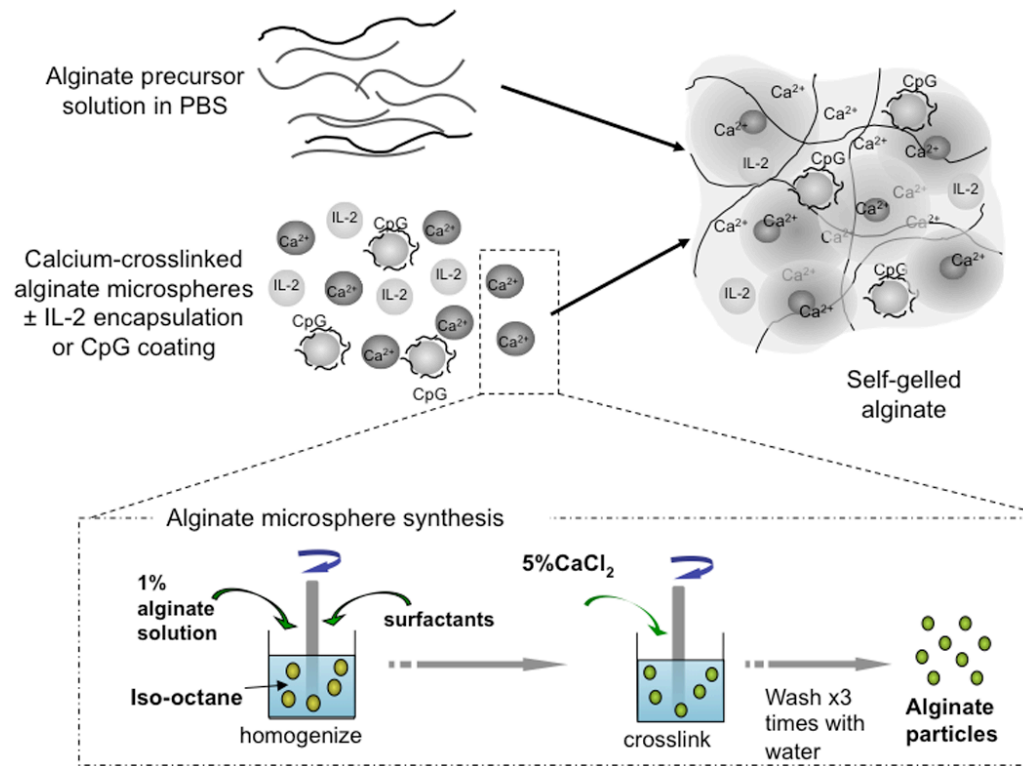
Figure 1. Schematic of self-gelling alginate formulations based on calcium reservoir alginate microspheres

Calcium-crosslinked alginate microspheres and microspheres modified with CpG oligonucleotides are mixed with soluble 'matrix' alginate in PBS containing soluble IL-2 (which may also contain cells or other factors). Diffusion of calcium ions in the microspheres into the surrounding solution induces crosslinking of the soluble alginate and gel formation. The inset figure outlines the process of calcium reservoir alginate microsphere synthesis via a water-in-oil emulsion of alginate in isooctane in the presence of surfactants.
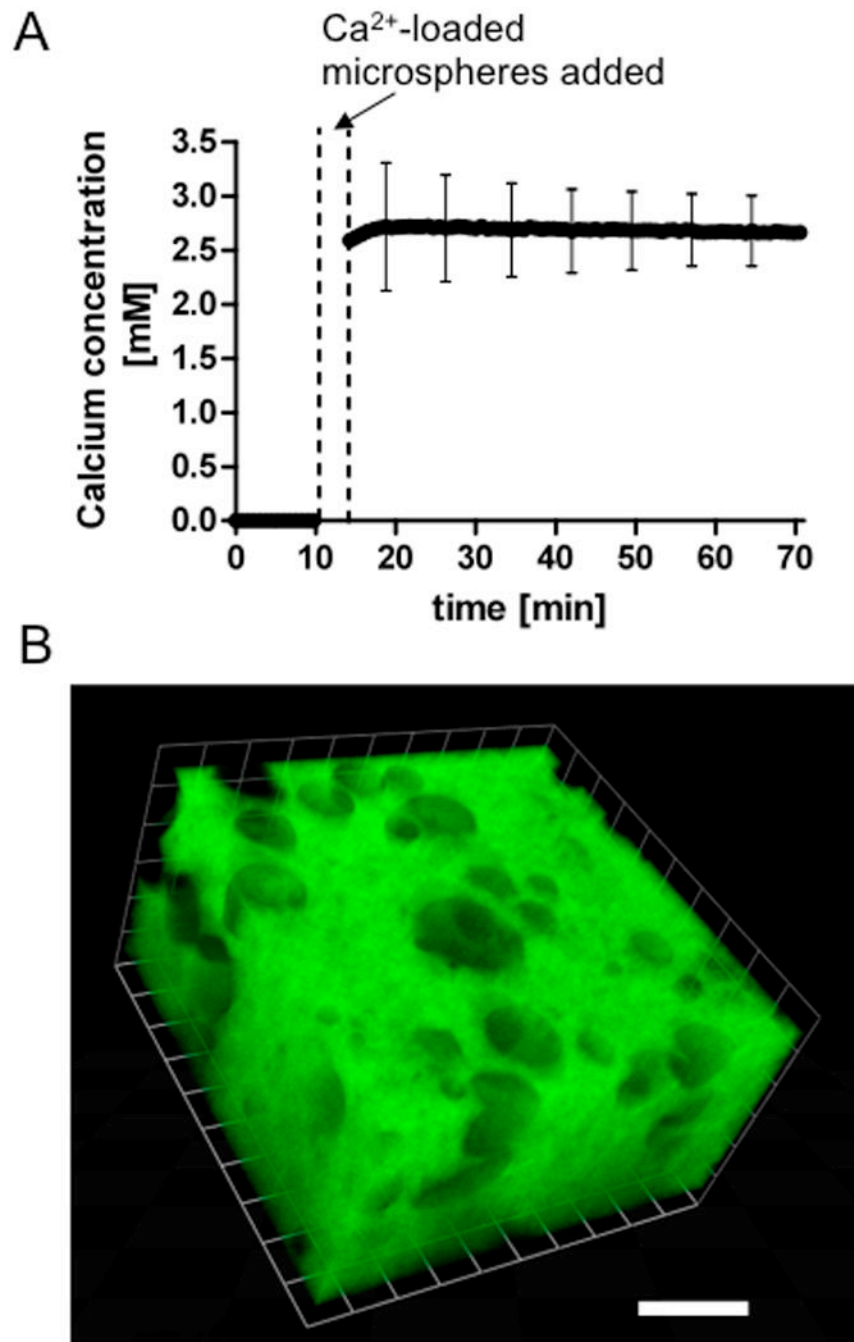
Figure 2. Calcium ions are rapidly released from calcium reservoir microspheres into the matrix alginate

(A) Temporal trace of calcium concentration in 'matrix' alginate determined by fluorescence microscopy using the calcium-sensitive dye mag-fura-2. Calcium reservoir microspheres (1.25×10^6) were mixed with 200 μL SLM20 alginate in PBS (composition used for injection *in vivo*) and immediately imaged in time-lapse microscopy. (Error bars = SD, every 10th timepoint). (B) 3D reconstruction of a self-gelling alginate formulation containing 4×10^6 calcium reservoir microspheres in 130μL SLM20 matrix (14.8 mM Ca^{2+} overall), showing alginate microspheres (nonfluorescent voids) distributed throughout the fluorescent matrix. (scale bar: 50μm).
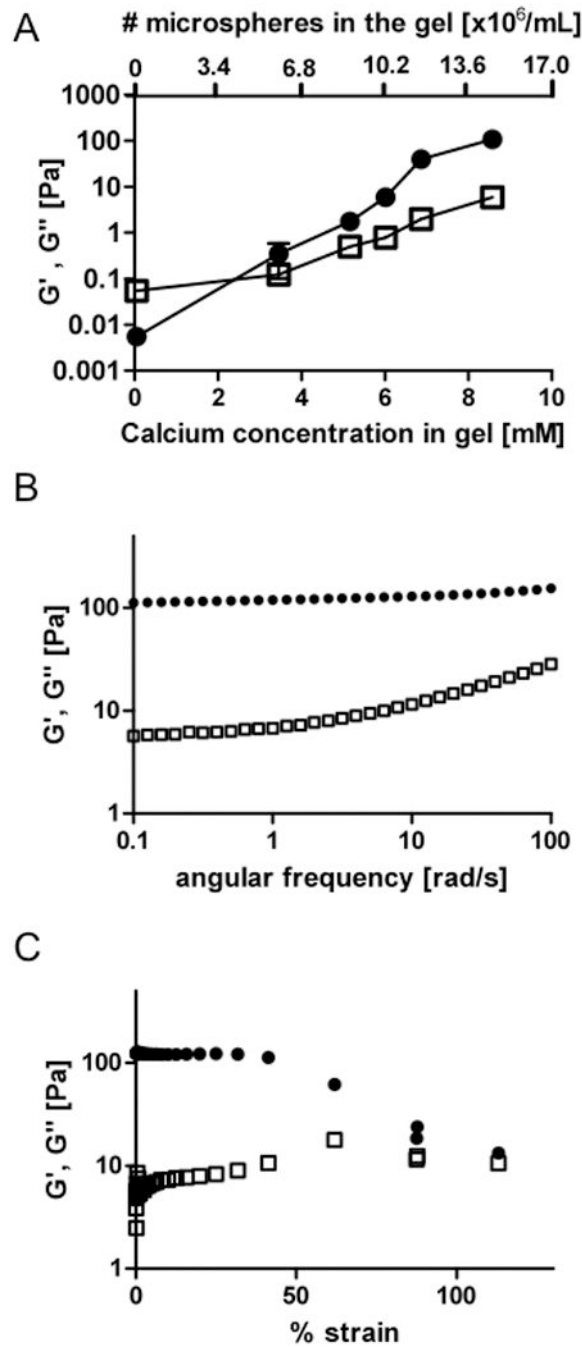
Figure 3. Mechanical properties of self-gelling alginate gels are controlled by the amount of calcium reservoir microspheres in the formulation
(A) Shear storage (G′ (●)) and loss (G″ (□)) moduli of self-gelled alginate containing different amounts of SLG20 microspheres were measured by parallel plate rheometer, showing an increase in the elastic shear moduli with the number of calcium reservoir alginate microspheres for a fixed total volume of the final gels. (B) Frequency sweep of self-gelling alginate gel with 8.6mM total calcium content shows the elastic component of the modulus G′ (●) dominating the mechanical behavior of the gel over the viscous component G″ (□) over two decades of angular frequency. (C) The magnitude of strain (5%) applied to the modulus measurement in fig 3A was in the linear region of the viscoelastic spectrum.

The plot shown is for the case of 8.6mM Ca^{2+} in a self-gelling alginate formulation ((G' (●)) and loss (G'' (□)).
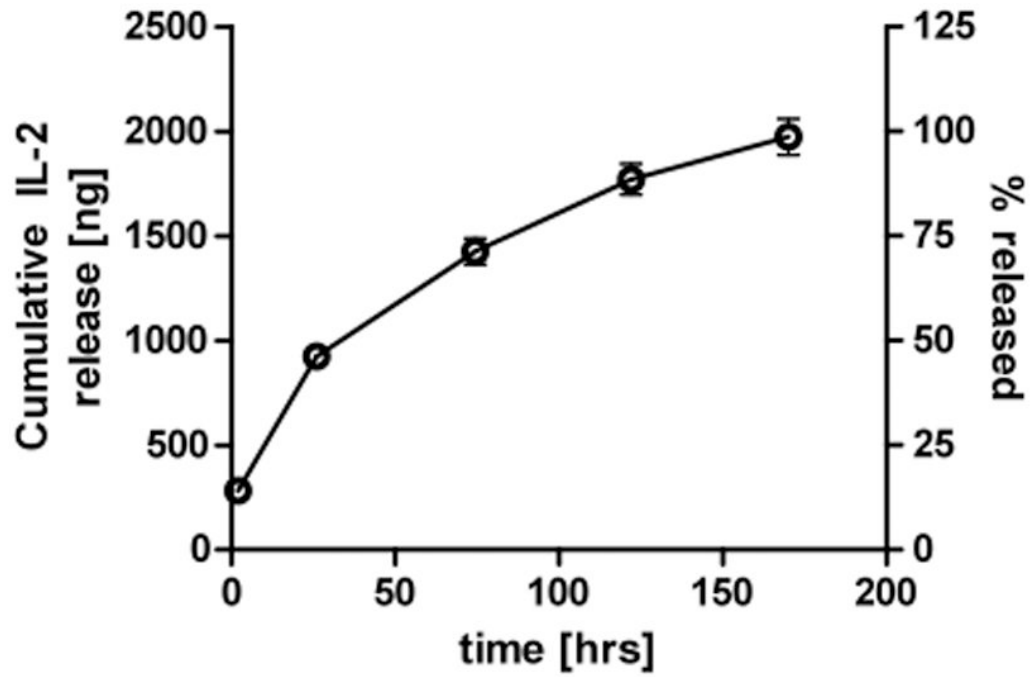
Figure 4. IL-2 loaded into self-gelling alginate is released in a sustained manner over a week *in vitro*
Cumulative release of IL-2, loaded into the self-gelling alginate formulation containing 11.1mM Ca^{2+}, as quantified by ELISA assay.
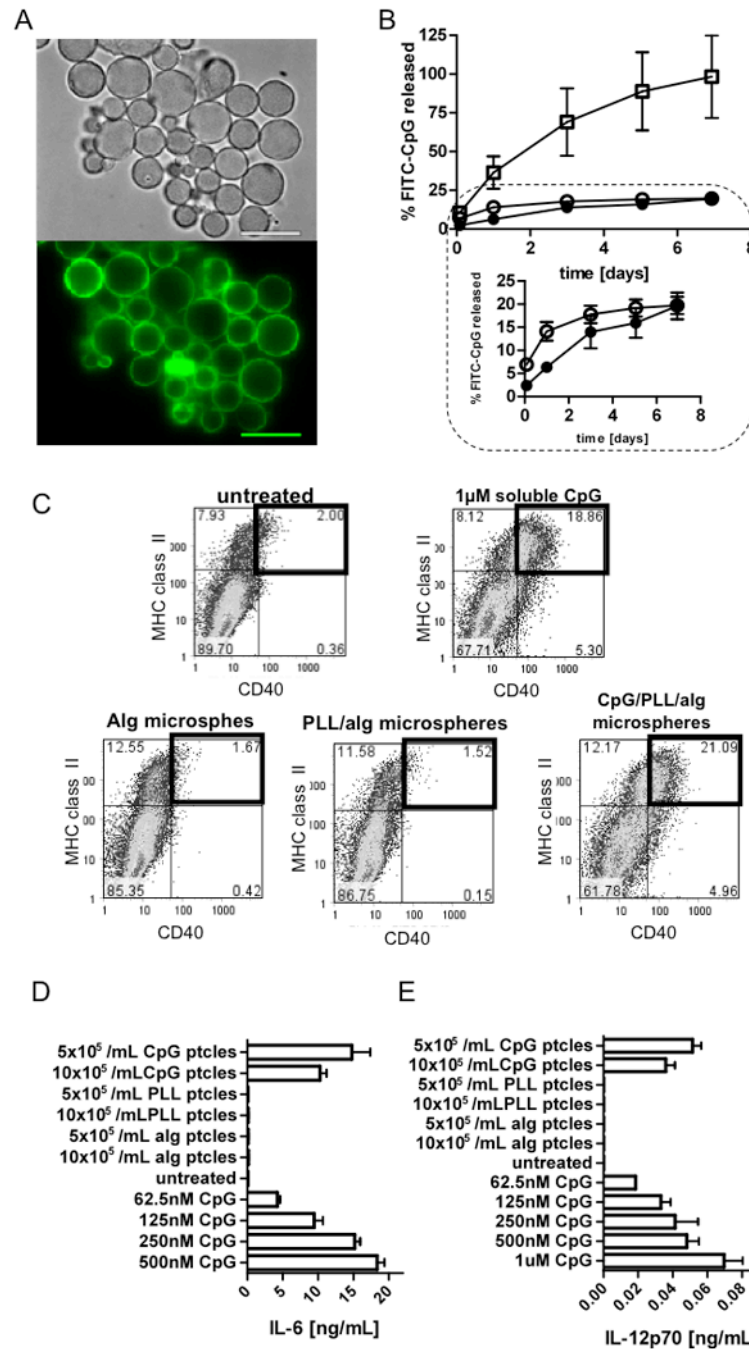
Figure 5. CpG oligonucleotide immobilization on alginate microspheres and activation of DCs by CpG-bearing microspheres

(A) Brightfield and fluorescence (FITC) micrographs of calcium reservoir microspheres coated with polylysine and FITC-CpG. (scale bars: 50μm). (B) Kinetics of FITC-CpG release from CpG/PLL/alginate particle suspensions (5 nmol FITC-CpG/10^6 microspheres) into serum-containing cell culture medium (○), CpG released from self-gelled alginate (11.1mM Ca^{2+}) containing the same number of CpG/PLL/alginate particles (●), or soluble CpG released from self-gelled alginate (11.1mM Ca^{2+}) encapsulating equivalent amounts of soluble CpG (□). (C) 1×10^6 bone marrow-derived dendritic cells (BMDCs) were incubated with $5-10\times10^5$ alginate microspheres, PLL/alginate microspheres, CpG/PLL/alginate

microspheres, or 1 μM soluble CpG (positive control), or were left untreated for 18 hrs, then analyzed for surface marker expression by flow cytometry. Shown are flow cytometry scatter plots of BMDCs gated on CD11c$^+$ cells, showing CD40 and MHC class II expression. Heavy boxes highlight highly mature (activated) CD40^{hi}MHC II^{hi} cells. CpG/PLL-coated microspheres were also able to trigger IL-6 (D) and IL-12p70 (E) secretions in BMDCs at least as efficiently as the soluble CpG did.
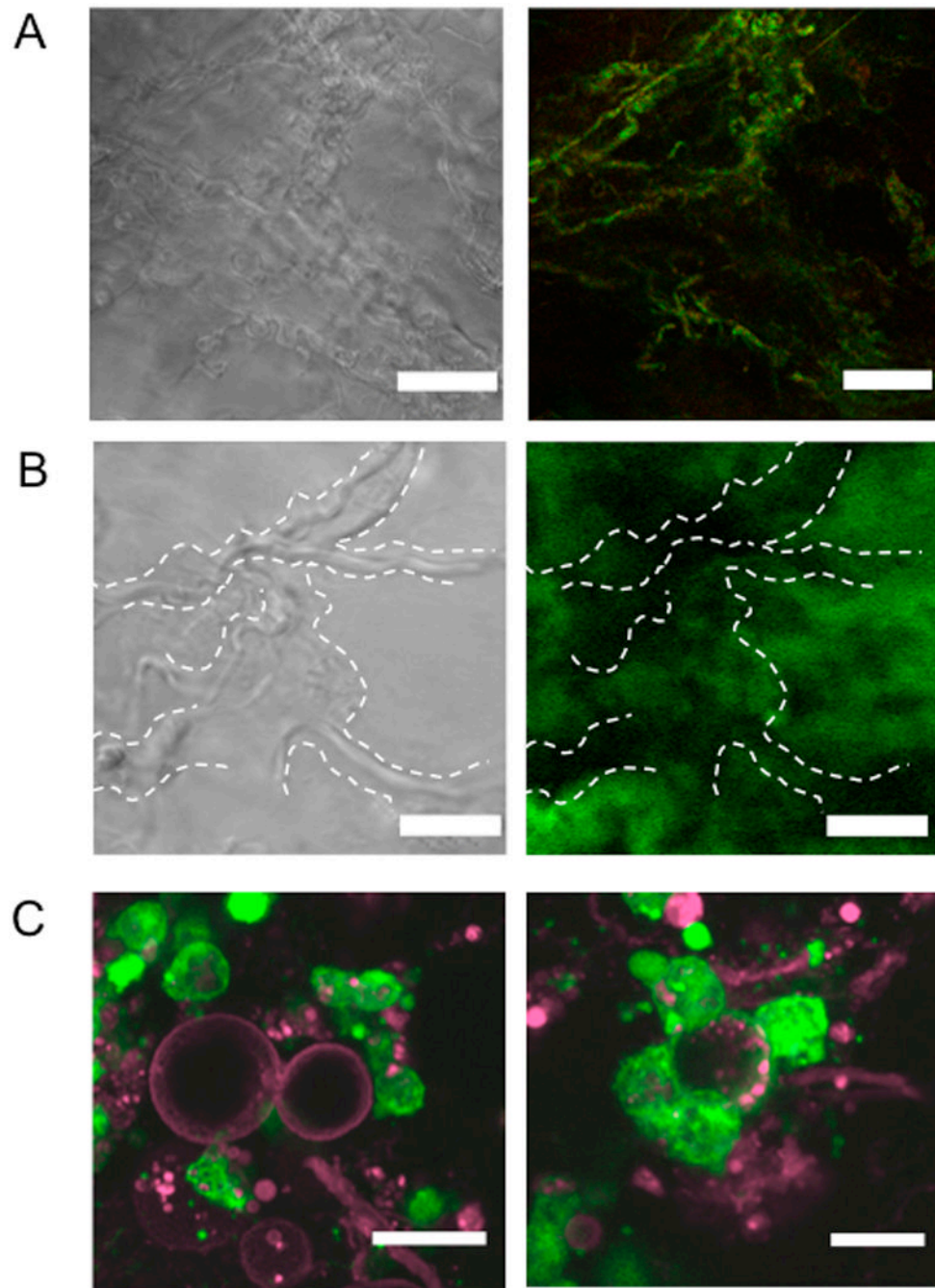
Figure 6. Self-gelling alginate structures and self-gelling alginate encapsulating Cy5-CpG/PLL-coated alginate microspheres *in vivo*
(A) Brightfield (left) and reflectance mode (right) images of self-gelling alginate ($\sim 9 \times 10^5$ microspheres in 150μL SLM20, 0.01g/mL) injected subcutaneously into back flanks of mice and explanted after 19 hrs shows micron-scale fibrils. (scale bars: 50μm). (B) Brightfield (left) and fluorescence confocal (right) images of self-gelling alginate with 6-aminofluorescein-labeled SLM20 reveals the fibrillar structures are not associated with alginate, indicating alginate forms macroporous gels when injected subcutaneously *in vivo*. (scale bars: 20μm). (C) Fluorescent Cy5-CpG (purple) on the surfaces of PLL-modified alginate microspheres was encapsulated into self-gelling alginate and injected into GFP+

mice. Cy5-CpG-coated microspheres are intact 48 hrs post-injection (left, scale bar:25 μm) and are accessible to infiltrating cells (right, shown in green, scale bar:15 μm) that can ingest the oligonucleotides. The micrographs are projections of z-planes over 6 μm.
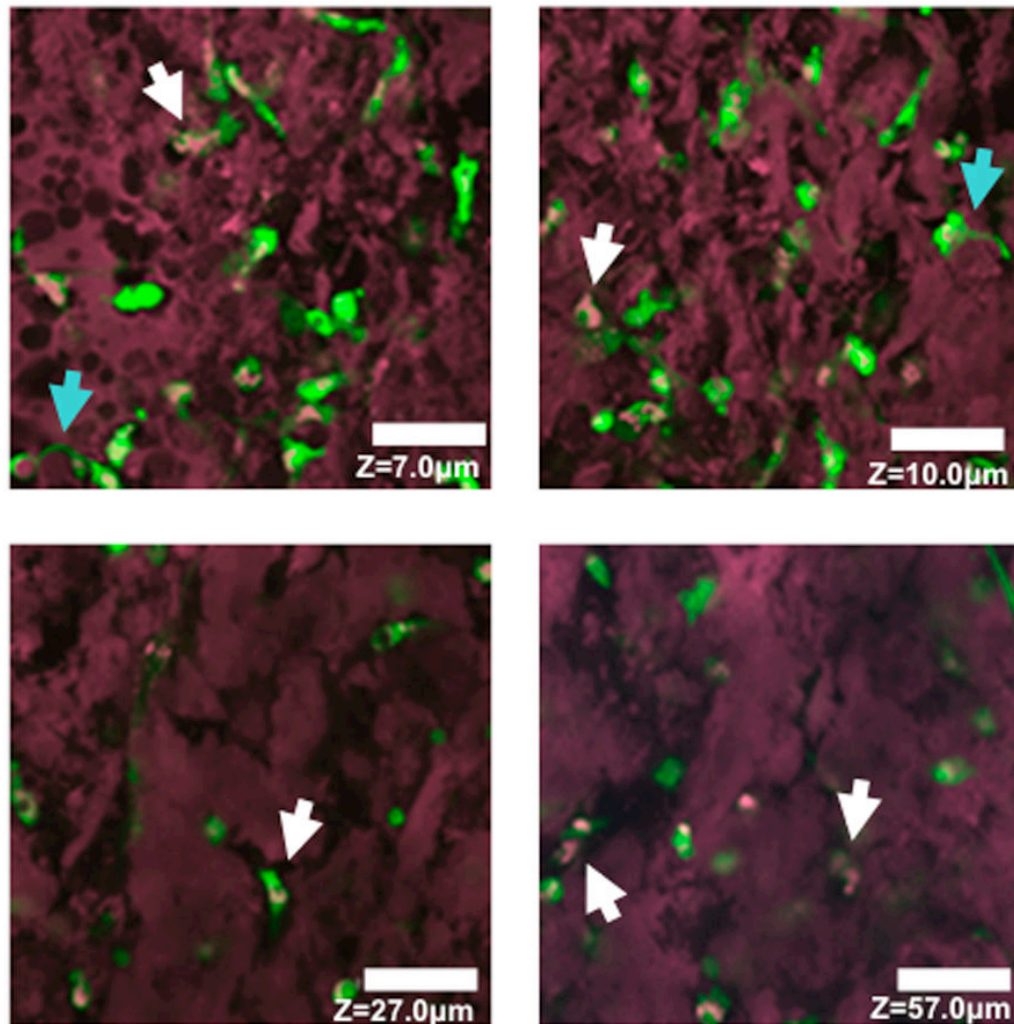
Figure 7. Host cells Infiltrate self-gelling alginate and preferentially occupy void spaces in the porous matrix
Fluorescence confocal microscope images of fluorescently labeled self-gelling alginate (purple) explanted from back flanks of mice 48 hrs after injection. Infiltrating GFP+ cells occupied void spaces in the macroporous gel structure and extended lamellipodia into void spaces (blue arrows), with some phagocytic cells having ingested the matrix alginate indicated by intracellular deposits of labeled alginate (white arrows). (scale bars: 50µm).

Table 1

Concentration of calcium ions in self-gelling alginate injected *in vivo* with or without calcium reservoir microspheres

Gel composition	Microsphere-derived Ca2+ [mM]	Total Ca^{2+} in explanted gels [mM]	Calculated Ca^{2+} contribution from interstitial fluid [mM]
no microspheres	0	5.5±0.5	5.5±0.5
with microspheres	3.7±0.3	8.1±1.3	4.5±0.2